ANL-7493

RETURN TO ANL (ICAHO) LIBRARY.

Argonne National Laboratory

STRENGTH-DEFORMATION CONSIDERATIONS OF AN INVOLUTE SHELL

by

A. H. Marchertas

The facilities of Argonne National Laboratory are owned by the United States Government. Under the terms of a contract (W-31-109-Eng-38) between the U. S. Atomic Energy Commission, Argonne Universities Association and The University of Chicago, the University employs the staff and operates the Laboratory in accordance with policies and programs formulated, approved and reviewed by the Association.

MEMBERS OF ARGONNE UNIVERSITIES ASSOCIATION

The University of Arizona
Carnegie-Mellon University
Case Western Reserve University
The University of Chicago
University of Cincinnati
Illinois Institute of Technology
University of Illinois
Indiana University
Iowa State University
The University of Iowa
Kansas State University
The University of Kansas
Loyola University
Marquette University
Michigan State University
The University of Michigan
University of Minnesota
University of Missouri
Northwestern University
University of Notre Dame
The Ohio State University
Ohio University
The Pennsylvania State University
Purdue University
Saint Louis University
Southern Illinois University
University of Texas
Washington University
Wayne State University
The University of Wisconsin

LEGAL NOTICE

This report was prepared as an account of Government sponsored work. Neither the United States, nor the Commission, nor any person acting on behalf of the Commission:

A. Makes any warranty or representation, expressed or implied, with respect to the accuracy, completeness, or usefulness of the information contained in this report, or that the use of any information, apparatus, method, or process disclosed in this report may not infringe privately owned rights; or

B. Assumes any liabilities with respect to the use of, or for damages resulting from the use of any information, apparatus, method, or process disclosed in this report.

As used in the above, "person acting on behalf of the Commission" includes any employee or contractor of the Commission, or employee of such contractor, to the extent that such employee or contractor of the Commission, or employee of such contractor prepares, disseminates, or provides access to, any information pursuant to his employment or contract with the Commission, or his employment with such contractor.

Printed in the United States of America
Available from
Clearinghouse for Federal Scientific and Technical Information
National Bureau of Standards, U. S. Department of Commerce
Springfield, Virginia 22151
Price: Printed Copy $3.00; Microfiche $0.65

ANL-7493
Reactor Technology

ARGONNE NATIONAL LABORATORY
9700 South Cass Avenue
Argonne, Illinois 60439

STRENGTH-DEFORMATION CONSIDERATIONS OF AN INVOLUTE SHELL

by

A. H. Marchertas

Reactor Engineering Division

April 1969

TABLE OF CONTENTS

LIST OF FIGURES

LIST OF TABLES

NOMENCLATURE

Symbol	Description	Units
a	Generating radius of the circular involute (see Fig. 4)	in.
$C_1, \ldots, C_6$	Constants of integration	
D	Flexural rigidity of shell	lb-in.
E	Modulus of elasticity of material	$lb/in.^2$
h	Thickness of shell	in.
M	Bending moment	lb-in./in.
M_p	Particular solution of bending moment [see Eq. (6)]	lb-in./in.
M_T	Bending moment due to thermal gradients	lb-in./in.
N	Membrane load	lb/in.
N_p	Particular solution of membrane load [see Eq. (3)]	lb/in.
N_T	Membrane load due to thermal gradients	lb/in.
p or $p(\theta)$	Average transverse pressure on shell walls	$lb/in.^2$
Q	Shear load	lb/in.
T or $T(z,\theta)$	Temperature distribution in shell	°F
u	Tangential deflection of shell	in.
u_p	Particular solution of tangential deflection	in.
w	Transverse deflection of shell	in.
w_p	Particular solution of transverse deflection	in.
z	Coordinate perpendicular to plane of shell (see Fig. 4)	
α	Coefficient of thermal expansion	$°F^{-1}$
ϵ	Strain in shell	in./in.
θ	Angular coordinate of shell (see Fig. 4)	rad
κ	Change in radius of curvature of shell	$in.^{-1}$
ν	Poisson's ratio	
ρ	Radius of curvature of shell	in.
σ	Stress in shell	$lb/in.^2$
ψ	Total subtended angle of the shell (see Fig. 4)	rad
$\chi(\theta)$	Some function of θ	

STRENGTH-DEFORMATION CONSIDERATIONS OF AN INVOLUTE SHELL

by

A. H. Marchertas

ABSTRACT

An exploratory analysis is made of the behavior of a thin, cylindrical, involute shell subjected to a steady-state pressure and internal thermal gradients (which vary along the involute). Five theoretical approaches are adapted to the one-variable, involute shell problem, and solved explicitly for the dependent variables of internal loads and displacements. Small-deflection theory is used throughout.

Each approach was used to solve two numerical problems, one involving uniform transverse pressure imposed on the shell, and the other subjecting it to isothermal expansion. In both problems, three boundary conditions were employed: fixed, pinned, and what is referred to as rotated edges. Quantitative differences between the respective solutions are discussed. Similar comparisons are made with available experimental data.

I. INTRODUCTION

During the period from March 1962 to September 1966, the fuel-development program in support of the Argonne Advanced Research Reactor (AARR)[1] was focussed on a fully enriched UO_2-stainless steel cermet, flat-plate core with an initial thermal output of 100 MW. In September 1966, a decision was made to revise the AARR concept to accommodate a graded U_3O_8-aluminum cermet, involute plate core. This core had been developed at Oak Ridge National Laboratory (ORNL) for their High Flux Isotope Reactor (HFIR).

Although the HFIR core was operational and performing satisfactorily at ORNL, the AARR core-design group at Argonne had no previous experience with graded, involute fuel plates. Moreover, the structural limitations of these plates under the adverse conditions anticipated in the AARR were unknown. Therefore, a stress-analysis study was initiated, the preliminary stages and results of which are described in this report.

Open literature on stress analysis of involute shells is essentially nonexistent. Moreover, to this author's knowledge, the only published work on involute fuel plates is predominantly experimentation performed in support of the HFIR core.[2,3] This lack of information is understandable since involute shapes are rarely encountered as structural elements. Therefore,

the analysis presented in this report pertains to a relatively simple involute shell problem and is based on small-deflection theory with one variable, that is, equilibrium conditions are established from the original shell geometry and the loads made independent of the displacements during loading. Also, the loads can be expressed in terms of integration constants to be evaluated from the boundary conditions.

However, in the process of this simple analysis, it was observed that variations existed in the final load-displacement relationships, and even small-deflection theory with one variable did not provide a unique solution. Since simple explicit resultant equations can be derived for the relevant variables, five theoretical solutions were obtained for purposes of comparison. The objectives here were: (1) to observe the typical variation between the different solutions, and (2) if appreciable, to select the most promising theory to be used in a more comprehensive analysis of the fuel plate. It was believed that more complicated problems should be analyzed only after the soundness of the simplest solution had been established.

Thus the simple involute shell problem treated in this report does not imply a solution to the actual fuel plate. The environmental conditions and plate composition are much more complicated than has been considered here for the steady-state condition. However, the results afford a better understanding of the involute plate behavior in general. This then may be taken as the first step in the general stress analysis of the involute fuel plate.

II. ANALYTICAL DEVELOPMENT

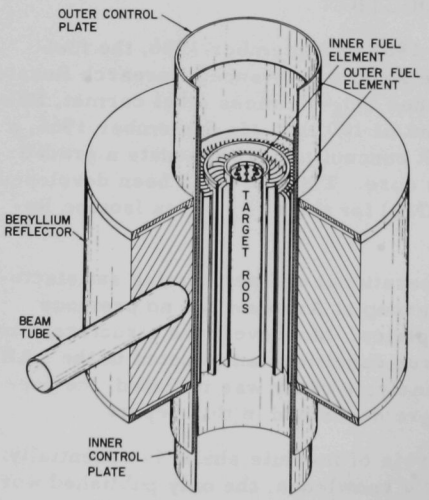

Fig. 1. Partial Section of HFIR Core Assembly

A. Description of HFIR

The HFIR was designed primarily to produce transuranium isotopes for use in the USAEC heavy-element research program. As shown in Fig. 1, the target rods containing ^{242}Pu and other transuranium isotopes are positioned vertically within a 5-in.-dia hole that forms the center of the reactor. Radially outward from this hole, the reactor is composed of two concentric fuel elements; two, thin, poison-bearing, concentric cylinders which serve as control plates; a concentric beryllium reflector (approximately 1 ft thick); and a water reflector of effectively infinite thickness. In the axial direction, the reactor is reflected by water.

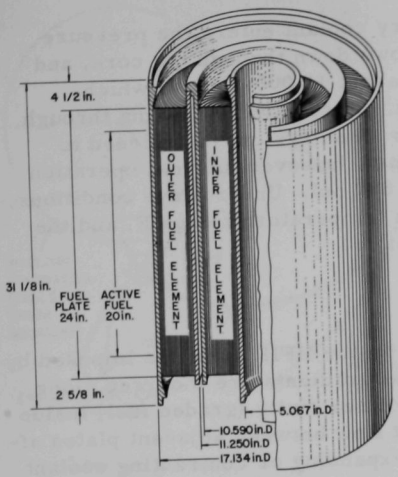

Fig. 2. Dimensional Characteristics of HFIR Fuel Elements

With reference to the fuel region (see Fig. 2) the inner element is 5.067 in. in ID and 10.590 in. in OD; it contains 171 fuel plates. The outer element is 11.250 in. in ID and 17.134 in. in OD; it contains 369 fuel plates. In both elements, the plates are 24 in. long (active length = 20 in.) and 0.05 in. thick; they are bent in the shape of an involute and welded to circular cylinders to form constant 0.05-in.-thick coolant channels. Before bending, the plates in the inner fuel element are approximately 3.6 in. wide and those in the outer fuel element are approximately 3.2 in. wide. As shown in Fig. 3, each plate is of a sandwich-type construction composed of U_3O_8-Al cermet fuel clad with Type 6061 aluminum. To reduce the radial peak-to-average power density ratio, the fuel is nonuniformly loaded along the arc of the involute. A burnable poison is included in the inner fuel element to flatten the neutron flux further and to reduce the negative reactivity requirements of the control plates. The control plates (see Fig. 1) are driven vertically in opposite directions by mechanisms located beneath the reactor vessel.

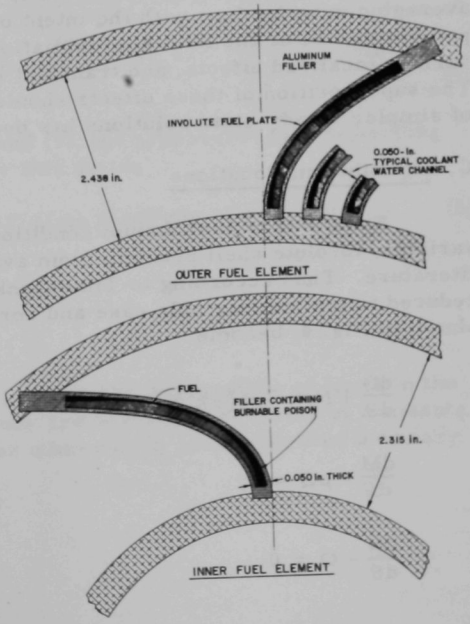

Fig. 3
Partial Plan View of Inner and Outer Fuel Elements Showing Distribution of Fuel and Burnable Poison in Fuel Plates

During reactor operation, primary coolant enters the pressure vessel at an elevation above the core, flows down through the core, and exits beneath the core. The flowrate is about 16,000 gpm, of which 13,000 gpm flows through the fuel region, the remainder flowing through the target, reflector, and control regions. The system is designed to operate at an inlet pressure up to 1,000 psi; however, normal operation at 100 MW requires an inlet pressure of 600 psi. Under these conditions, the inlet temperature is 120°F, the outlet temperature is 164°F, and the pressure drop through the core is 100 psi.

B. Nature of Imposed Loads

Operating loads on the fuel plates in the HFIR core are imposed by thermal gradients and pressure. Thermal gradients are incurred along the length of the plates by the variations of reactivity (graded fuel) inside the plates and the degree to which coolant flow between adjacent plates affects the situation. Pressure due to the expanding or contracting coolant provides the external transverse pressure on the fuel plates. The boundaries also come into play insofar as they resist radial expansion or contraction of the plates.

In response to the imposed loads, adjacent fuel plates may flex toward or away from each other, and the load parameters will change accordingly. This is a coupled transient phenomena, and a true analytical representation of all relevant effects is very difficult. Therefore, some averaging must be done with the intent of approximating the important design parameters. For the first approximation, changes in plate properties, various localized effects, and transient loading in general can be neglected. The superposition of these effects should be considered after the soundness of simpler steady-state solutions has been ensured.

C. Equilibrium Equations

Equations of equilibrium conditions can be adapted to the one-variable, involute shell problem from available expressions in the open literature. Thus according to Timoshenko,[4] the equilibrium conditions, when reduced to the one-variable case and corrected to the coordinate system shown in Fig. 4, become

$$\frac{dQ}{d\theta} + N = -\rho p(\theta); \tag{1a}$$

$$\frac{dM}{d\theta} - \rho Q = 0; \tag{1b}$$

$$\frac{dN}{d\theta} - Q = 0. \tag{1c}$$

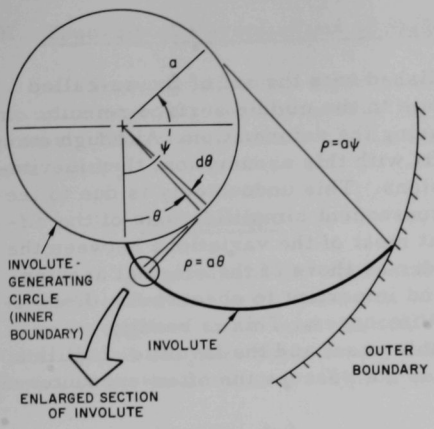

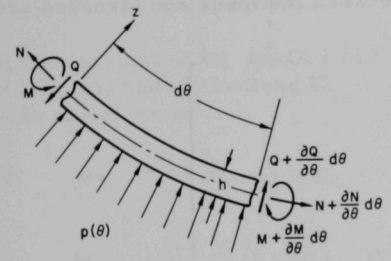

Fig. 4. Model and Nomenclature Used in Analysis of the One-variable Involute Shell

Substitution of Eq. (1c) into Eq. (1a) yields a second-order ordinary differential equation with one unknown dependent variable N:

$$N + \frac{d^2N}{d\theta^2} = -a\theta p(\theta), \tag{2}$$

for which the standard solution is

$$N = C_1 \sin\theta + C_2 \cos\theta + N_p. \tag{3}$$

The membrane load N_p is the particular solution of Eq. (2) and can be represented mathematically by

$$N_p = \frac{1}{2i}\left\{e^{i\theta}\int e^{-i\theta}\chi(\theta)\,d\theta - e^{-i\theta}\int e^{i\theta}\chi(\theta)\,d\theta\right\}, \tag{4}$$

where

$$\chi(\theta) = -a\theta p(\theta).$$

From Eqs. (1c) and (3), the expression for the shear load becomes

$$Q = C_1 \cos\theta - C_2 \sin\theta + \frac{d}{d\theta}(N_p). \tag{5}$$

Similarly, from Eqs. (1b) and (5), the expression for the bending moment is obtained by integration; this yields

$$M = C_1 a(\cos\theta + \theta\sin\theta) - C_2 a(\sin\theta - \theta\cos\theta) + C_3 + M_p, \tag{6}$$

where

$$M_p = a\int \theta \frac{d}{d\theta}(N_p)\,d\theta.$$

Thus Eqs. (3), (5), and (6) provide the expressions of loads in the involute plate shown in Fig. 4. They are expressed in terms of constants of integration and will be evaluated numerically from specified boundary conditions.

D. Load-deformation Relationships

These relationships are established with the aid of the so-called Love-Kirchhoff assumption that normals to the middle surface remain straight, normal, and inextensional during the deformation. Although many authors in the literature on shells start with this assumption, they inevitably end up with different final expressions. This undoubtedly is due to the rigor of the subsequent analysis and consequent simplifications of the differential equations. Koiter[5] states that most of the variations between the different solutions are of the same order as those of the original assumption. Nevertheless, it is interesting and important to observe the discrepancies in terms of typical numerical differences. This is readily accomplished by means of a one-variable case, and the involute shell is a convenient configuration because it does not possess the often-encountered property of symmetry.

Accordingly, the relationships between the loads and stresses are given by

$$\left.\begin{aligned} N &= \int_{-h/2}^{h/2} \sigma \, dz, \\ M &= \int_{-h/2}^{h/2} \sigma z \, dz, \end{aligned}\right\} \tag{7}$$

and the stress-strain relationship in a plane by

$$\sigma = \frac{E}{1-\nu^2}[\epsilon - (1+\nu)\alpha T(z,\theta)]. \tag{8}$$

Strain-displacements relations have been derived by Love[6] and, due to the assumptions involved, are linear functions of the thickness coordinate z. Typically,

$$\epsilon = \frac{1}{\rho}\frac{du}{d\theta} + \frac{1}{1-(z/\rho)}\frac{w}{\rho} - \frac{z}{1-(z/\rho)}\kappa, \tag{9}$$

where κ is the change in shell curvature and is expressed in a variety of ways.

Change in shell curvature is the main variable discussed in subsequent sections of this report. Also discussed is the assumption that the ratio z/ρ is very much smaller than unity and is therefore neglected.*

*Omission of the ratio z/ρ is used by Novozhilov[7] as a criterion to differentiate thin shells as opposed to thick shells.

E. Theoretical Formulations of Shell Curvature

Since the different equations of κ are the results of many approaches, no advantage is gained by presenting the individual solutions in any specific order. Thus the equations cited are given in the order in which they were analyzed.

1. Timoshenko

Timoshenko's[4] approach in deriving the expression for change in shell curvature is an extension of the method used in the study of ordinary strength of materials. In addition, he utilizes the concept of inextensibility and assumes that, during deformation, the radius of curvature is reduced by the amount w. This approach yields

$$\kappa = \frac{1}{\rho^2} \frac{d}{d\theta}\left(u + \frac{dw}{d\theta}\right). \tag{10}$$

He also assumes that $z/\rho \ll 1$ in Eq. (9). Therefore, on substituting Eq. (9) into Eq. (8) and performing the integrations of Eq. (7), the expressions for loads are given by

$$N = \frac{12D}{ah^2\theta}\left(\frac{du}{d\theta} - w\right) - N_T; \tag{11a}$$

$$M = -\frac{D}{a^2\theta^2} \frac{d}{d\theta}\left(u + \frac{dw}{d\theta}\right) - M_T, \tag{11b}$$

where

$$N_T = \frac{\alpha E}{1 - \nu} \int_{-h/2}^{h/2} T(z,\theta)\, dz;$$

$$M_T = \frac{\alpha E}{1 - \nu} \int_{-h/2}^{h/2} zT(z,\theta)\, dz.$$

Solving for u in Eq. (11b) and substituting it into Eq. (11a) results in a second-order differential equation of the form

$$w + \frac{d^2w}{d\theta^2} = -\frac{a^2\theta}{D}\left[\frac{h^2}{12a}(N + N_T) + \theta(M + M_T)\right]. \tag{12}$$

Substitution of Eqs. (3) and (6) into Eq. (12) and solving it yields the following expression for transverse deflection of the shell:

$$w = \frac{a^3\theta}{48D}\left[\left(30 - \frac{h^2}{a^2}\right)(\sin\theta - \theta\cos\theta) - 2\theta^2(10\sin\theta - 3\theta\cos\theta)\right] C_1$$

$$+ \frac{a^3\theta}{48D}\left[\left(30 - \frac{h^2}{a^2}\right)(\cos\theta + \theta\sin\theta) - 2\theta^2(10\cos\theta + 3\theta\sin\theta)\right] C_2$$

$$- \frac{a^2}{D}(\theta^2 - 2)\, C_3 + C_4 \sin\theta + C_5 \cos\theta + w_p, \qquad (13)$$

where

$$w_p = \frac{1}{2i}\left\{e^{i\theta}\int e^{-i\theta}\chi(\theta)\, d\theta - e^{-i\theta}\int e^{i\theta}\chi(\theta)\, d\theta\right\}$$

and

$$\chi(\theta) = \frac{a^2\theta}{D}\left[\frac{h^2}{12a}(N_p + N_T) + \theta(M_p + M_T)\right].$$

The slope, or first derivative of w, also can be used to evaluate some of the boundary conditions. On differentiation, Eq. (13) yields

$$\frac{dw}{d\theta} = \frac{a^3}{48D}\left[\left(30 - \frac{h^2}{a^2}\right)(\sin\theta - \theta\cos\theta + \theta^2\sin\theta)\right.$$

$$\left. - 2\theta^2(30\sin\theta - 2\theta\cos\theta + 3\theta^2\sin\theta)\right] C_1$$

$$+ \frac{a^3}{48D}\left[\left(30 - \frac{h^2}{a^2}\right)(\cos\theta + \theta\sin\theta + \theta^2\cos\theta)\right.$$

$$\left. - 2\theta^2(30\cos\theta + 2\theta\sin\theta + 3\theta^2\cos\theta)\right] C_2$$

$$- \frac{2a^2}{D}\theta C_3 + C_4\cos\theta - C_5\sin\theta + \frac{d}{d\theta}(w_p). \qquad (14)$$

The tangential displacement u is related to w in Eq. (11b) and ready for straightforward solution in conjunction with Eq. (6). This gives

$$u = -\frac{a^3}{48D}\left[\left(30 - \frac{h^2}{a^2}\right)(\sin\theta - \theta\cos\theta + \theta^2\sin\theta)\right.$$

$$\left. + 2\theta^2(66\sin\theta - 22\theta\cos\theta - 3\theta^2\sin\theta) - 384(\sin\theta - \theta\cos\theta)\right] C_1$$

$$-\frac{a^3}{48D}\left[\left(30 - \frac{h^2}{a^2}\right)(\cos\theta + \theta\sin\theta + \theta^2\cos\theta)\right.$$

$$\left. + 2\theta^2(66\cos\theta + 22\theta\sin\theta - 3\theta^2\cos\theta) - 384(\cos\theta + \theta\sin\theta)\right] C_2$$

$$-\frac{a^2\theta}{3D}(\theta^2 - 6)\,C_3 - C_4\cos\theta + C_5\sin\theta + C_6 + u_p, \qquad (15)$$

where

$$u_p = -\frac{d}{d\theta}(w_p) - \frac{a^2}{D}\int \theta^2(M_p + M_T)\,d\theta.$$

This completes the solution of the one-variable involute shell by Timoshenko's formulation. Equations (3), (5), and (6) give the loads in terms of the integration constants C_1, C_2, and C_3. Equations (13), (14), and (15) give the deflections in the same terms, and the additional constants C_4, C_5, and C_6. At this point, the solution is ready for numerical evaluation. Since six constants of integration are to be evaluated, and there are two ends of the shell, three boundary conditions must be specified for a complete solution of the problem.

2. Modified Timoshenko

The assumptions of Timoshenko in deriving his expression for κ are not really necessary if the definition of strain is used in the derivation. As given by Timoshenko, the basic definition of the change in curvature is

$$\kappa = \frac{d\theta + \Delta d\theta}{ds + \Delta ds} - \frac{1}{\rho},$$

where s is the arc length, ρ the radius of curvature, and Δ the increment involved. If the terms of the equation are expressed as follows:

$$\Delta d\theta = \frac{d^2w}{ds^2}\,ds;$$

$$d\theta = \frac{1}{\rho}\,ds;$$

$$\Delta ds = \epsilon\,ds,$$

substituted into the original equation, and the secondary terms are cancelled, then

$$\kappa = \frac{1}{1+\epsilon}\left[\frac{1}{\rho}+\frac{1}{\rho}\frac{d}{d\theta}\left(\frac{1}{\rho}\frac{dw}{d\theta}\right)\right] - \frac{1}{\rho},$$

which, on use of the binomial expansion, can be rewritten as

$$\kappa = \frac{1}{\rho}\left[1 + \frac{d}{d\theta}\left(\frac{1}{\rho}\frac{dw}{d\theta}\right)\right](1 - \epsilon + \epsilon^2 - \ldots) - \frac{1}{\rho}.$$

The relationship between the strain and displacements, also given by Timoshenko, is

$$\epsilon = \frac{1}{\rho}\left(\frac{du}{d\theta} - w\right).$$

Thus on performing the substitution, expanding, and finally neglecting secondary terms, an approximation for the change in curvature is given by

$$\kappa = \frac{1}{\rho}\left[\frac{d}{d\theta}\left(\frac{1}{\rho}\frac{dw}{d\theta}\right) - \frac{1}{\rho}\left(\frac{du}{d\theta} - w\right)\right]. \tag{16}$$

Equation (16) can now be used, as before, to yield load-displacement relationships. Hence, neglecting the terms z/ρ in Eq. (9), using it in Eqs. (7) in conjunction with Eq. (16), and adapting the result to the involute shell, we obtain

$$N = \frac{12D}{ah^2\theta}\left(\frac{du}{d\theta} - w\right) - N_T; \tag{17a}$$

$$M = -\frac{D}{a^2\theta}\left[\frac{d}{d\theta}\left(\frac{1}{\theta}\frac{dw}{d\theta}\right) - \frac{1}{\theta}\left(\frac{du}{d\theta} - w\right)\right] - M_T. \tag{17b}$$

Substitution of the term $\frac{1}{\theta}\left(\frac{du}{d\theta} - w\right)$ from Eq. (17a) into Eq. (17b) results in an equation involving only w. Hence,

$$\frac{d}{d\theta}\left(\frac{1}{\theta}\frac{dw}{d\theta}\right) = \frac{a^2}{D}\left[\frac{h^2}{12a}(N + N_T) - \theta(M + M_T)\right]. \tag{18}$$

On performing the indicated integration and multiplying the result by θ, the following expression for the slope is obtained:

$$\frac{dw}{d\theta} = -\frac{a^3\theta}{D}\left[3(\cos\theta + \theta\sin\theta) - \left(\theta^2 - \frac{h^2}{12a^2}\right)\cos\theta\right] C_1$$

$$+\frac{a^3\theta}{D}\left[3(\sin\theta - \theta\cos\theta) - \left(\theta^2 - \frac{h^2}{12a^2}\right)\sin\theta\right] C_2$$

$$-\frac{a^2\theta^3}{2D} C_3 + a\theta C_4 + \frac{d}{d\theta}(w_p), \qquad (19)$$

where

$$w_p = \frac{a^2}{D}\int \theta \int\left[\frac{h^2}{12a}(N_p + N_T) - \theta(M_p + M_T)\right] d\theta\, d\theta.$$

Integration of Eq. (19) results in the transverse deflection formula

$$w = -\frac{a^3}{D}\left[\left(15 + \frac{h^2}{12a^2}\right)(\cos\theta + \theta\sin\theta) - \theta^2(6\cos\theta + \theta\sin\theta)\right] C_1$$

$$+\frac{a^3}{D}\left[\left(15 + \frac{h^2}{12a^2}\right)(\sin\theta - \theta\cos\theta) - \theta^2(6\sin\theta - \theta\cos\theta)\right] C_2$$

$$-\frac{a^2\theta^4}{8D} C_3 + \frac{a\theta^2}{2} C_4 + C_5 + w_p. \qquad (20)$$

Equation (20) thus completes the relationships required for the boundary value problem.

3. Koiter

In deriving his load-displacement relationships, Koiter[5] used a method of differential geometry as formulated for this purpose by Reissner.[8] In this manner the change of curvature became

$$\kappa = \frac{1}{\rho}\frac{d}{d\theta}\left[\frac{1}{\rho}\left(u + \frac{dw}{d\theta}\right)\right]. \qquad (21)$$

Thus on substituting Eq. (21) into Eq. (9) and neglecting the terms z/ρ, the expressions for loads can be obtained as in the previous sections. In this case

$$N = \frac{12D}{ah^2\theta}\left(\frac{du}{d\theta} - w\right) - N_T; \tag{22a}$$

$$M = -\frac{D}{a^2\theta}\frac{d}{d\theta}\left[\frac{1}{\theta}\left(u + \frac{dw}{d\theta}\right)\right] - M_T. \tag{22b}$$

Substitution of the solution for Eq. (22a) into Eq. (22b) results in a second-order differential equation for u:

$$\frac{d}{d\theta}\left[\frac{1}{\theta}\left(u + \frac{d^2u}{d\theta^2}\right)\right] = \frac{a^2}{D}\left[\frac{h^2}{12a}\frac{d}{d\theta}\left\{\frac{1}{\theta}\frac{d}{d\theta}\left[\theta(N + N_T)\right]\right\} - \theta(M + M_T)\right]. \tag{23}$$

Further substitution of Eqs. (3) and (6) into Eq. (23) and performance of the indicated integrations result in an algebraic equation for u:

$$\begin{aligned} u = &-\frac{a^3\theta}{8D}\left[15(\cos\theta + \theta\sin\theta) - \theta^2(6\cos\theta + \theta\sin\theta)\right. \\ &\left. + \frac{h^2}{6a^2}(\cos\theta - \theta\sin\theta)\right] C_1 \\ &+ \frac{a^3\theta}{8D}\left[15(\sin\theta - \theta\cos\theta) - \theta^2(6\sin\theta - \theta\cos\theta)\right. \\ &\left. + \frac{h^2}{6a^2}(\sin\theta + \theta\cos\theta)\right] C_2 \\ &- \frac{a^2\theta}{2D}(\theta^2 - 6)\,C_3 + \theta C_4 + C_5\sin\theta + C_6\cos\theta + u_p, \end{aligned} \tag{24}$$

where

$$u_p = \frac{1}{2i}\left\{e^{i\theta}\int e^{-i\theta}\chi(\theta)\,d\theta - e^{-i\theta}\int e^{i\theta}\chi(\theta)\,d\theta\right\}$$

and

$$\chi(\theta) = \frac{a^2}{D}\left\{\frac{h^2}{12a}\frac{d}{d\theta}\left[\theta(N_p + N_T)\right] - \theta\int\theta(M_p + M_T)\,d\theta\right\}.$$

If the expression for w obtained from Eq. (22a) is differentiated and solved in conjunction with Eq. (24), the transverse deflection formula becomes

$$w = -\frac{a^3}{8D}\left[15(\cos\theta + \theta\sin\theta) - \theta^2(3\cos\theta - 2\theta\sin\theta + \theta^2\cos\theta)\right.$$

$$\left. + \frac{h^2}{6a^2}(\cos\theta + \theta\sin\theta - \theta^2\cos\theta)\right] C_1$$

$$+\frac{a^3}{8D}\left[15(\sin\theta - \theta\cos\theta) - \theta^2(3\sin\theta + 2\theta\cos\theta + \theta^2\sin\theta)\right.$$

$$\left. + \frac{h^2}{6a^2}(\sin\theta - \theta\cos\theta - \theta^2\sin\theta)\right] C_2$$

$$-\frac{3a^2}{2D}(\theta^2 - 2)C_3 + C_4 + C_5\cos\theta - C_6\sin\theta + w_p, \qquad (25)$$

where

$$w_p = \frac{d}{d\theta}(u_p) - \frac{ah^2\theta}{12D}(N_p + N_T).$$

Differentiation of Eq. (25) yields the slope of the elastic curve:

$$\frac{dw}{d\theta} = -\frac{a^3\theta}{8D}\left[9(\cos\theta + \theta\sin\theta) - \theta^2(2\cos\theta - \theta\sin\theta)\right.$$

$$\left. - \frac{h^2}{6a^2}(\cos\theta - \theta\sin\theta)\right] C_1$$

$$+\frac{a^3\theta}{8D}\left[9(\sin\theta - \theta\cos\theta) - \theta^2(2\sin\theta + \theta\cos\theta)\right.$$

$$\left. - \frac{h^2}{6a^2}(\sin\theta + \theta\cos\theta)\right] C_2$$

$$-\frac{3a^2}{D}\theta C_3 - C_5\sin\theta - C_6\cos\theta + \frac{d}{d\theta}(w_p). \qquad (26)$$

This concludes the one-variable involute shell analysis using Koiter's equations.

4. Flügge

The approach of Flügge[9] in deriving the expression for change in shell curvature is similar to that of Timoshenko, except it excludes the

assumption of inextensibility. Also, it does not provide for the component in the change of curvature due to the tangential displacement u. Accordingly, his expression is

$$\kappa = \frac{1}{\rho^2}\frac{d^2w}{d\theta^2}. \tag{27}$$

In the further development of the load-displacement relations Flügge does not assume that $z/\rho \ll 1$. Thus, Eq. (9), as defined, is used in conjunction with Eqs. (8) and (7) to obtain

$$N = \frac{D}{\rho}\left[\frac{12}{h^2}\left(\frac{du}{d\theta} - w\right) - \frac{1}{\rho^2}\left(w + \frac{d^2w}{d\theta^2}\right)\right] - N_T; \tag{28a}$$

$$M = -\frac{D}{\rho^2}\left(w + \frac{d^2w}{d\theta^2}\right) - M_T, \tag{28b}$$

where adjustment to proper sign convention is incorporated.

In the process of integrating Eq. (9) logarithmic terms were encountered. In his development, Flügge expanded the logarithms in powers of h/ρ, and neglected the fifth and higher powers to yield Eqs. (28) for the one-variable case. According to Flügge, neglecting the higher powers meant only that the rigidity D in these formulas was slightly modified, the differences being of the order h^2/ρ^2.

Equation (28b) is in terms of w alone and explicit solution for w is obtained by direct integration of

$$w + \frac{d^2w}{d\theta^2} = -\frac{a^2\theta^2}{D}(M + M_T). \tag{29}$$

Thus on substituting Eq. (6) into Eq. (29) and solving it,

$$\begin{aligned} w = {} & \frac{a^3\theta}{24D}[15(\sin\theta - \theta\cos\theta) - \theta^2(10\sin\theta - 3\theta\cos\theta)]\, C_1 \\ & + \frac{a^3\theta}{24D}[15(\cos\theta + \theta\sin\theta) - \theta^2(10\cos\theta + 3\theta\sin\theta)]\, C_2 \\ & - \frac{a^2}{D}(\theta^2 - 2)\, C_3 + C_4\sin\theta + C_5\cos\theta + w_p, \end{aligned} \tag{30}$$

where

$$w_p = \frac{1}{2i}\left\{e^{i\theta}\int e^{-i\theta}\chi(\theta)\, d\theta - e^{-i\theta}\int e^{i\theta}\chi(\theta)\, d\theta\right\}$$

and

$$\chi(\theta) = -\frac{a^2\theta^2}{D}(M_p + M_T).$$

The slope, or first derivative of w, becomes

$$\frac{dw}{d\theta} = \frac{a^3}{24D}\left[15(\sin\theta - \theta\cos\theta - \theta^2\sin\theta) + \theta^3(2\cos\theta - 3\theta\sin\theta)\right] C_1$$

$$+ \frac{a^3}{24D}\left[15(\cos\theta + \theta\sin\theta - \theta^2\cos\theta) - \theta^3(2\sin\theta + 3\theta\cos\theta)\right] C_2$$

$$- \frac{2a^2\theta}{D} C_3 + C_4\cos\theta - C_5\sin\theta + \frac{d}{d\theta}(w_p). \qquad (31)$$

Since the tangential displacement u is related to w by Eq. (28a), substituting Eq. (6) into it and solving result in

$$u = \frac{a^3}{24D}\left[177(\sin\theta - \theta\cos\theta) - \theta^2(81\sin\theta - 22\theta\cos\theta)\right.$$

$$\left. + \left(3\theta^4 - 2\frac{h^2}{a^2}\right)\sin\theta\right] C_1$$

$$+ \frac{a^3}{24D}\left[177(\cos\theta + \theta\sin\theta) - \theta^2(81\cos\theta + 22\theta\sin\theta)\right.$$

$$\left. + \left(3\theta^4 - 2\frac{h^2}{a^2}\right)\cos\theta\right] C_2$$

$$- \frac{a^2\theta}{3D}\left(\theta^2 - 6 + \frac{h^2}{4a^2}\right) C_3 - C_4\cos\theta + C_5\sin\theta + C_6 + u_p, \qquad (32)$$

where

$$u_p = \int\left\{w_p + \frac{h^2}{12D}\left[a\theta(N_p + N_T) - (M_p + M_T)\right]\right\} d\theta.$$

Equation (32) completes the expressions for the deformations of Flügge's formulation and the boundary value problem is ready for solution.

5. Miller

In deriving the relationships between loads and displacements Miller[10] used the differential geometry and obtained a somewhat different expression for κ:

$$\kappa = \frac{1}{\rho}\left[\frac{d}{d\theta}\left(\frac{1}{\rho}\frac{dw}{d\theta}\right) - \frac{u}{\rho^2}\frac{d\rho}{d\theta}\right]. \tag{33}$$

Similar to Flügge, Miller also retains all terms in Eq. (9) and integrates the complete expression. As a result, the load-displacement relations become

$$N = \frac{12D}{ah^2\theta}\left\{\frac{du}{d\theta} - w + C^*\left[w - \frac{u}{\theta} + \theta\frac{d}{d\theta}\left(\frac{1}{\theta}\frac{dw}{d\theta}\right)\right]\right\} - N_T; \tag{34a}$$

$$M = \frac{12D}{h^2}C^*\left[w - \frac{u}{\theta} + \theta\frac{d}{d\theta}\left(\frac{1}{\theta}\frac{dw}{d\theta}\right)\right] - M_T, \tag{34b}$$

where

$$C^* = 1 - \frac{a\theta}{h}\ln\left(\frac{2a\theta + h}{2a\theta - h}\right).$$

When Eq. (34b) is solved for u and substituted into Eq. (34a),

$$\frac{d}{d\theta}\left(w + \frac{d^2w}{d\theta^2}\right) = \frac{h^2}{12D}\left[a(N + N_T) - \frac{1}{\theta}\left(1 + \frac{\theta}{C^{*2}}\frac{dC^*}{d\theta} - \frac{1}{C^*}\right)(M + M_T)\right.$$

$$\left. + \frac{1}{C^*}\frac{d}{d\theta}(M + M_T)\right]. \tag{35}$$

Equation (35) is in terms of trigonometric and logarithmic functions, and evaluation of u as before becomes almost impossible. However, the logarithmic functions can be approximated by a few terms of infinite expansions, as was done by Flügge in his derivations. When adapted to the individual logarithmic terms of Eq. (35), these approximations become*

$$1 + \frac{\theta}{C^{*2}}\frac{dC^*}{d\theta} - \frac{1}{C^*} = \frac{36a^2\theta^2}{h^2}; \qquad \frac{1}{C^*} = 1 - \frac{12a^2\theta^2}{h^2}. \tag{36}$$

On introduction of these approximations, Eq. (35) becomes

$$\frac{d}{d\theta}\left(w + \frac{d^2w}{d\theta^2}\right) = \frac{h^2}{12D}\left[a(N + N_T) - \frac{36a^2\theta}{h^2}(M + M_T)\right.$$

$$\left. + \left(1 - \frac{12a^2\theta^2}{h^2}\right)\frac{d}{d\theta}(M + M_T)\right], \tag{37}$$

*The expressions for the regular logarithmic expansions have been modified slightly to make the limiting value of the quantity (at $\theta = 0$) correspond to unity.

which yields

$$w = -\frac{a^3\theta}{8D}\left[3(5\sin\theta - \theta\cos\theta) + \theta^2(2\sin\theta - \theta\cos\theta)\right.$$

$$\left. - \frac{h^2}{6a^2}(\sin\theta - \theta\cos\theta)\right] C_1$$

$$-\frac{a^3\theta}{8D}\left[3(5\cos\theta + \theta\sin\theta) + \theta^2(2\cos\theta + \theta\sin\theta)\right.$$

$$\left. - \frac{h^2}{6a^2}(\cos\theta + \theta\sin\theta)\right] C_2$$

$$-\frac{3a^2}{2D}(\theta^2 - 2)\, C_3 + C_4 + C_5\sin\theta + C_6\cos\theta + w_p, \qquad (38)$$

where

$$w_p = \frac{1}{2i}\left\{e^{i\theta}\int e^{-i\theta}\chi(\theta)\, d\theta - e^{-i\theta}\int e^{i\theta}\chi(\theta)\, d\theta\right\}$$

and

$$\chi(\theta) = \frac{a^2}{D}\int\left[\frac{h^2}{12a}(N_p + N_T) - 3\theta(M_p + M_T)\right.$$

$$\left. + \left(\frac{h^2}{12a^2} - \theta^2\right)\frac{d}{d\theta}(M_p + M_T)\right] d\theta.$$

The slope of the elastic curve becomes

$$\frac{dw}{d\theta} = -\frac{a^3}{8D}\left[3(5\sin\theta + 3\theta\cos\theta + 3\theta^2\sin\theta) - \theta^3(2\cos\theta - \theta\sin\theta)\right.$$

$$\left. - \frac{h^2}{6a^2}(\sin\theta - \theta\cos\theta + \theta^2\sin\theta)\right] C_1$$

$$-\frac{a^3}{8D}\left[3(5\cos\theta - 3\theta\sin\theta + 3\theta^2\cos\theta) + \theta^3(2\sin\theta + \theta\cos\theta)\right.$$

$$\left. - \frac{h^2}{6a^2}(\cos\theta + \theta\sin\theta + \theta^2\cos\theta)\right] C_2$$

$$-\frac{3a^2\theta}{D}\, C_3 + C_5\cos\theta - C_6\sin\theta + \frac{d}{d\theta}(w_p). \qquad (39)$$

The tangential displacement u is obtained by using Eq. (34b) in conjunction with Eq. (36). Subsequent integration gives

$$u = \frac{a^3}{8D}\left[15(\sin\theta - \theta\cos\theta - \theta^2\sin\theta) + \theta^3(6\cos\theta + \theta\sin\theta)\right.$$

$$\left. - \frac{h^2}{6a^2}(\sin\theta + 3\theta\cos\theta + \theta^2\sin\theta)\right] C_1$$

$$+ \frac{a^3}{8D}\left[15(\cos\theta + \theta\sin\theta - \theta^2\cos\theta) - \theta^3(6\sin\theta - \theta\cos\theta)\right.$$

$$\left. - \frac{h^2}{6a^2}(\cos\theta - 3\theta\sin\theta + \theta^2\cos\theta)\right] C_2$$

$$- \frac{a^2\theta}{2D}\left(\theta^2 - 6 + \frac{h^2}{6a^2}\right) C_3 + \theta C_4 - C_5\cos\theta + C_6\sin\theta + u_p, \qquad (40)$$

where

$$u_p = \theta\chi(\theta) - \frac{d}{d\theta}(w_p) - \frac{a^2\theta}{D}\left(\frac{h^2}{12a^2} - \theta^2\right)(M_p + M_T).$$

Equation (40) completes the one-variable involute shell analysis using Miller's formulation.

In summary, Table 1 lists the five equations for curvature κ as adapted to the one-variable involute shell.

TABLE I

EQUATIONS OF CURVATURE κ USED IN DERIVING LOAD-DISPLACEMENT RELATIONS IN THE ONE-VARIABLE INVOLUTE SHELL

FORMULATION	κ
FLÜGGE	$\frac{1}{\rho^2}\frac{d^2w}{d\theta^2}$
KOITER	$\frac{1}{\rho}\frac{d}{d\theta}\left[\frac{1}{\rho}\left(u + \frac{dw}{d\theta}\right)\right]$
MILLER	$\frac{1}{\rho}\left[\frac{d}{d\theta}\left(\frac{1}{\rho}\frac{dw}{d\theta}\right) - \frac{1}{\rho^2}u\frac{d\rho}{d\theta}\right]$
MODIFIED TIMOSHENKO	$\frac{1}{\rho}\left[\frac{d}{d\theta}\left(\frac{1}{\rho}\frac{dw}{d\theta}\right) - \frac{1}{\rho}\left(\frac{du}{d\theta} - w\right)\right]$
TIMOSHENKO	$\frac{1}{\rho^2}\frac{d}{d\theta}\left(u + \frac{dw}{d\theta}\right)$

III. NUMERICAL COMPARISON OF SOLUTIONS

Two simple numerical examples were employed for the purpose of comparing the individual formulations, using the one-variable mathematical model. In the first example, the shell was acted upon by a constant, uniform, transverse pressure with no thermal gradients. In the second example, the shell was subjected to a constant isothermal expansion with no applied pressure between the stationary boundaries. Table 2 lists, in terms of constant p and T, the particular solutions of the various differential equations derived in Sect. II.

Both examples were subdivided into three parts, each distinguished by the type of boundary conditions assumed. The first boundary condition, usually referred to as the pinned edges, is mathematically represented by

$$w\Big|_{\theta=0} = u\Big|_{\theta=0} = M\Big|_{\theta=0} = w\Big|_{\theta=\psi} = u\Big|_{\theta=\psi} = M\Big|_{\theta=\psi} = 0. \qquad (41)$$

The second, identified as the fixed boundary condition, is represented by

$$w\Big|_{\theta=0} = u\Big|_{\theta=0} = \frac{dw}{d\theta}\Big|_{\theta=0} = w\Big|_{\theta=\psi} = u\Big|_{\theta=\psi} = \frac{dw}{d\theta}\Big|_{\theta=\psi} = 0. \qquad (42)$$

The third boundary condition treated was the so-called "rotated" edges. Here, both ends of the shell are fixed in the regular sense, but are allowed to rotate relative to each other and with respect to the center of the involute circle (see Fig. 4). Mathematically, this boundary condition is represented by

$$w\Big|_{\theta=0} = u\Big|_{\theta=0} = \frac{dw}{d\theta}\Big|_{\theta=0} = u\Big|_{\theta=\psi} - \psi w\Big|_{\theta=\psi} = Q\Big|_{\theta=\psi} - \psi N\Big|_{\theta=\psi} = \frac{dw}{d\theta}\Big|_{\theta=\psi} = 0. \qquad (43)$$

The dimensional, material, and load parameters used in the sample solutions were:

$a = 2.72$ in.	$E = 1 \times 10^7$ psi
$h = 0.039$ in.	$\nu = 0.3$
$\psi = 1.636$ rad	$\alpha = 1.3 \times 10^{-5}\ ^\circ F^{-1}$
$p = 10.51$ psi	$T = 100^\circ F$

In the first boundary conditions considered, T was assumed to be zero. In the second, p was assumed to be zero. These input parameters were selected to facilitate comparison between analysis and experiment as described later in this report (see Sect. IV).

TABLE 2
PARTICULAR SOLUTIONS OF THE DIFFERENTIAL EQUATIONS

SYMBOL / FORMULATION	N_p	M_p	w_p	$\frac{d}{d\theta} w_p$	u_p
FLÜGGE	$-ap\theta$	$-\frac{1}{2}a^2 p\theta^2$	$\frac{a^4 p}{2D}\left(\theta^4 - 12\theta^2 + 24\right)$	$\frac{2a^4 p\theta}{D}\left(\theta^2 - 6\right)$	$\frac{a^4 p\theta}{2D}\left[\frac{1}{5}\theta^4 - \theta^2\left(4 + \frac{h^2}{18a^2}\right) + 24\right] + \frac{1}{2}a\alpha(1+\nu)T\theta^2$
KOITER	"	"	$\frac{a^4 p}{2D}\left[\frac{5}{4}\left(\theta^4 - 12\theta + 24\right) + \frac{h^2}{6a^2}\left(\theta^2 - 2\right)\right] - a\alpha(1+\nu)T\theta$	$\frac{a^4 p\theta}{2D}\left[5\left(\theta^2 - 6\right) + \frac{h^2}{3a^2}\right] - a\alpha(1+\nu)T$	$\frac{a^4 p\theta}{2D}\left[\frac{1}{4}\left(\theta^4 - 20\theta^2 + 120\right) - \frac{h^2}{3a^2}\right] + a\alpha(1+\nu)T$
MILLER	"	"	$\frac{a^4 p}{8D}\left[5\theta^4 - 60\theta^2 + 120 - \frac{2h^2}{3a^2}\left(\theta^2 - 2\right)\right] + a\alpha(1+\nu)T\theta$	$\frac{a^4 p\theta}{2D}\left(5\theta^2 - 30 - \frac{h^2}{3a^2}\right) + a\alpha(1+\nu)T$	$\frac{a^4 p\theta}{8D}\left[\theta^4 - 20\theta^2 + 120 - \frac{1}{3}\left(\theta^2 - 4\right)\frac{h^2}{a^2}\right] + a\alpha(1+\nu)T\left(\theta^2 - 1\right)$
MODIFIED TIMOSHENKO	"	"	$\frac{a^4 p\theta^4}{96D}\left(2\theta^2 - \frac{h^2}{a^2}\right) + \frac{1}{3}a\alpha(1+\nu)T\theta^3$	$\frac{a^4 p\theta^3}{24D}\left(3\theta^2 - \frac{h^2}{a^2}\right) + a\alpha(1+\nu)T\theta^2$	$\frac{a^4 p\theta^3}{48D}\left[\frac{\theta^4}{7} - \left(\frac{\theta^2}{10} + \frac{4}{3}\right)\frac{h^2}{a^2}\right] + \frac{1}{12}a\alpha(1+\nu)T\theta^2\left(\theta^2 + 6\right)$
TIMOSHENKO	"	"	$\frac{a^4 p}{12D}\left[6\theta^4 - \left(\theta^2 - 2\right)\left(72 - \frac{h^2}{a^2}\right)\right] - a\alpha(1+\nu)T\theta$	$\frac{a^4 p\theta}{6D}\left(12\theta^2 - 72 + \frac{h^2}{a^2}\right) - a\alpha(1+\nu)T$	$\frac{a^4 p\theta}{30D}\left[3\theta^2\left(\theta^2 - 20\right) + 5\left(72 - \frac{h^2}{a^2}\right)\right] + a\alpha(1+\nu)T$

Each of Eqs. (41) through (43) provides a total of six conditions--three for each end of the shell. When the relevant equations of Sect. II are subjected to these conditions, six simultaneous algebraic equations result. Each equation was programmed for a matrix solution in which the individual coefficients of the matrix could be put in separately. The combined programs thus provide numerical values of the dependent variables w, u, N, M, and Q at different values of the independent variable θ along the length of the shell as the final output. This permits the plotting of each of them, as in Figs. 5 through 10.

These graphs show the relative variations in each parameter for the five theoretical solutions evaluated. In most solutions, the variation of one function with the independent variable θ is quite similar (amplitude provides the pertinent source of comparison). The few exceptions are instances where the slope of the function varies with θ from solution to solution and thus the configuration is not exactly the same. A good illustration of this is the displacement configuration for the pinned-edge-boundary condition in both examples. The tangential displacement for the isothermal load condition, in particular, exhibits the most marked deviation in configuration.

Theoretically, the more rigorous the analytical approach, the more accurate the results, other conditions remaining equal. However, the validity of this statement depends also on the accuracy of the original assumptions. Koiter[5] points out that most of the refinements encountered in shell literature are of the same order of magnitude as are the errors attributable to the basic assumptions. Therefore, he presents a set of equations for the theory of shells in as simple a form as is consistent with the original assumptions. In addition, at least for the one-variable case, his solution coincides with that of Love,[6] Novoshilov,[7] Reisser,[8] and Sanders,[11] to name a few. It is on this basis that Koiter's solution was chosen as a reference for numerical comparison with the other four solutions.

Table 3 lists for both sample problems the percentage of deviations at maximum values of the dependent variables employed in the solutions. Where appearing, the minus sign indicates the value is less than that given in the Koiter solution. (Accuracy of the tabulated values is within 0.1%.)

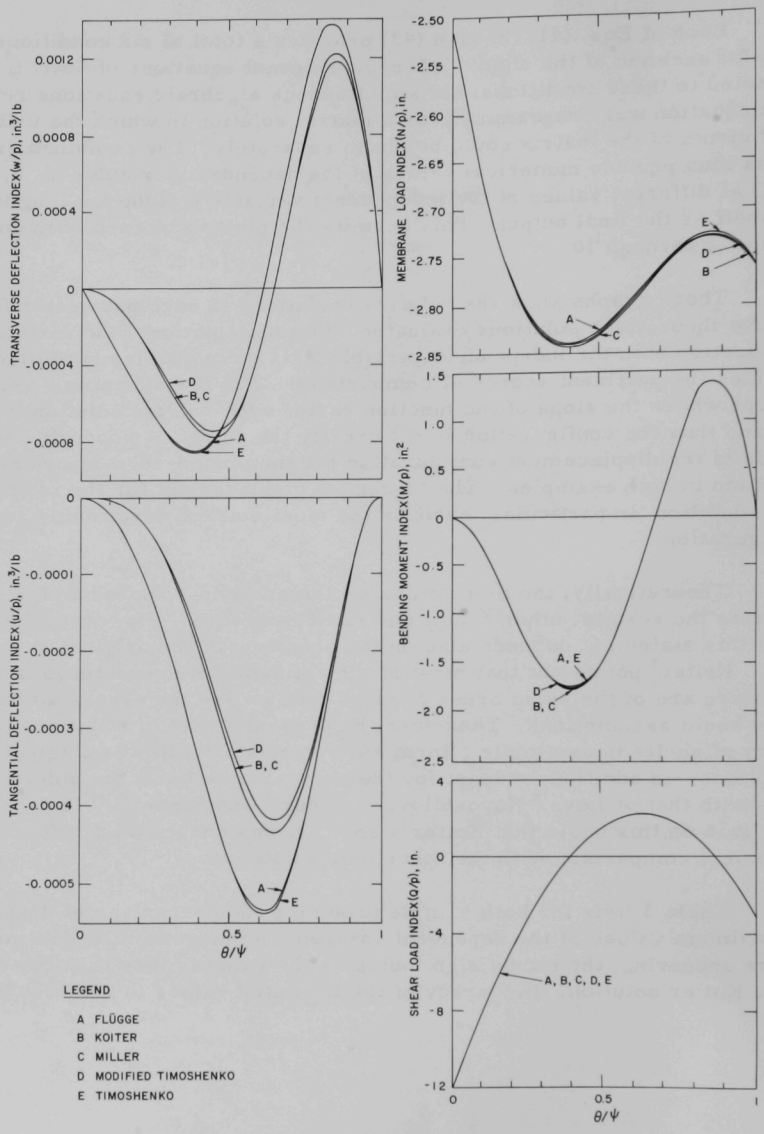

Fig. 5. Variation in Displacement and Internal Load of Involute Shell Which Has Pinned End Supports and Is Subjected to Uniform Pressure

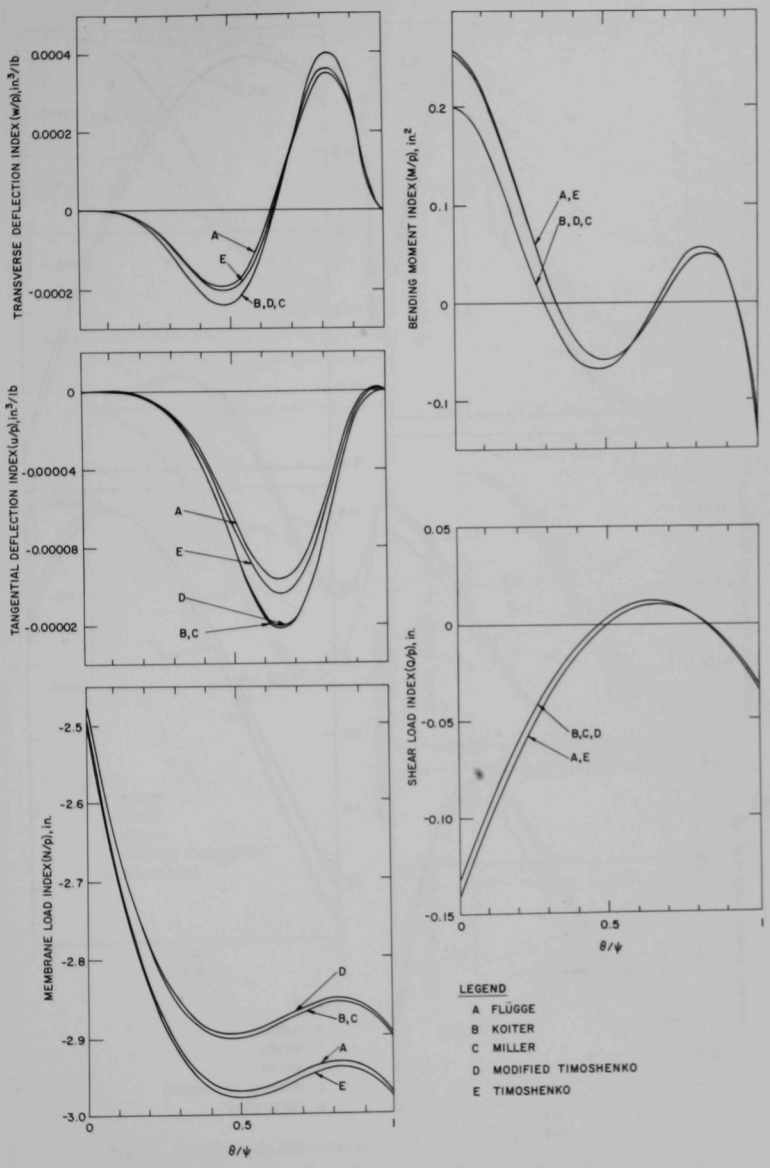

Fig. 6. Variation in Displacement and Internal Load of Involute Shell Which Has Fixed End Supports and Is Subjected to Uniform Pressure

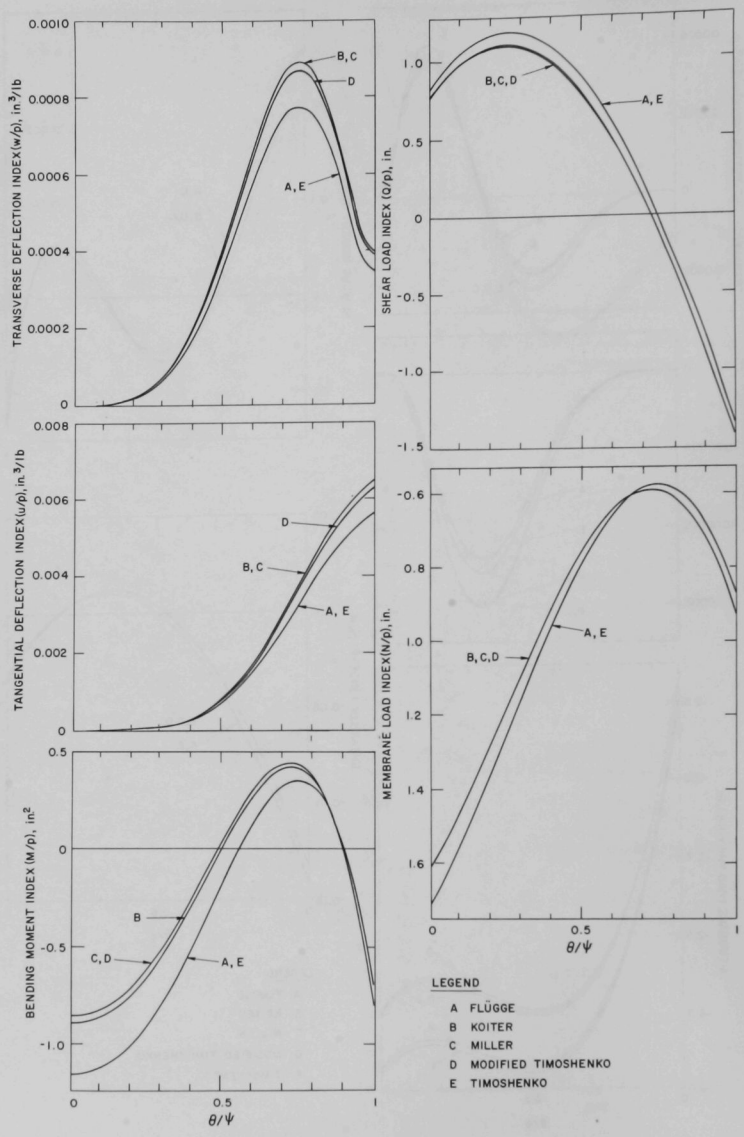

Fig. 7. Variation in Displacement and Internal Load of Involute Shell Which Has Rotated End Supports and Is Subjected to Uniform Pressure

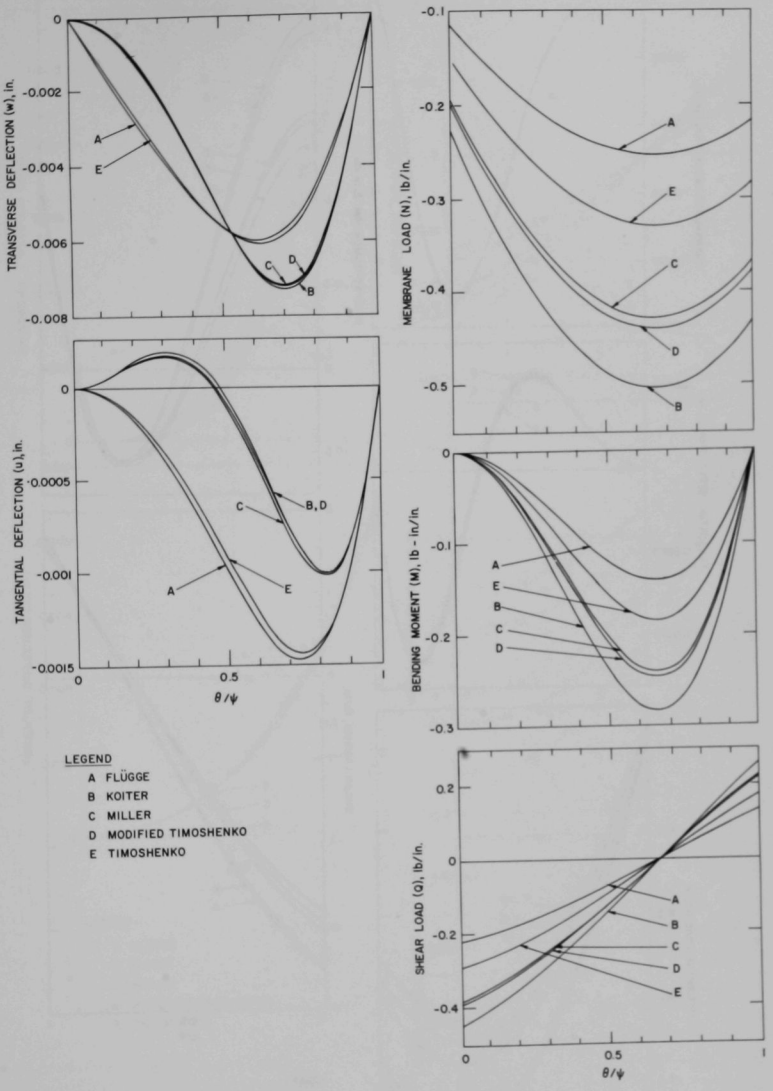

Fig. 8. Variation in Displacement and Internal Load of Involute Shell Which Has Pinned End Supports and Is Subjected to Isothermal Expansion

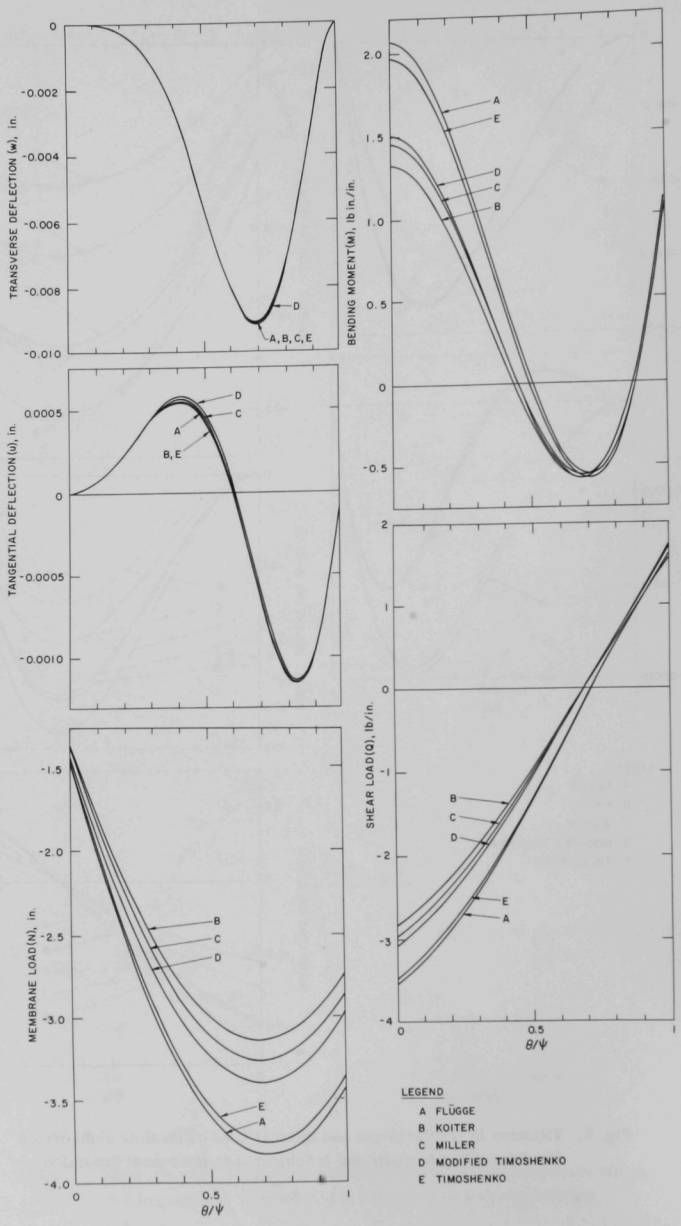

Fig. 9. Variation in Displacement and Internal Load of Involute Shell Which Has Fixed End Supports and Is Subjected to Isothermal Expansion

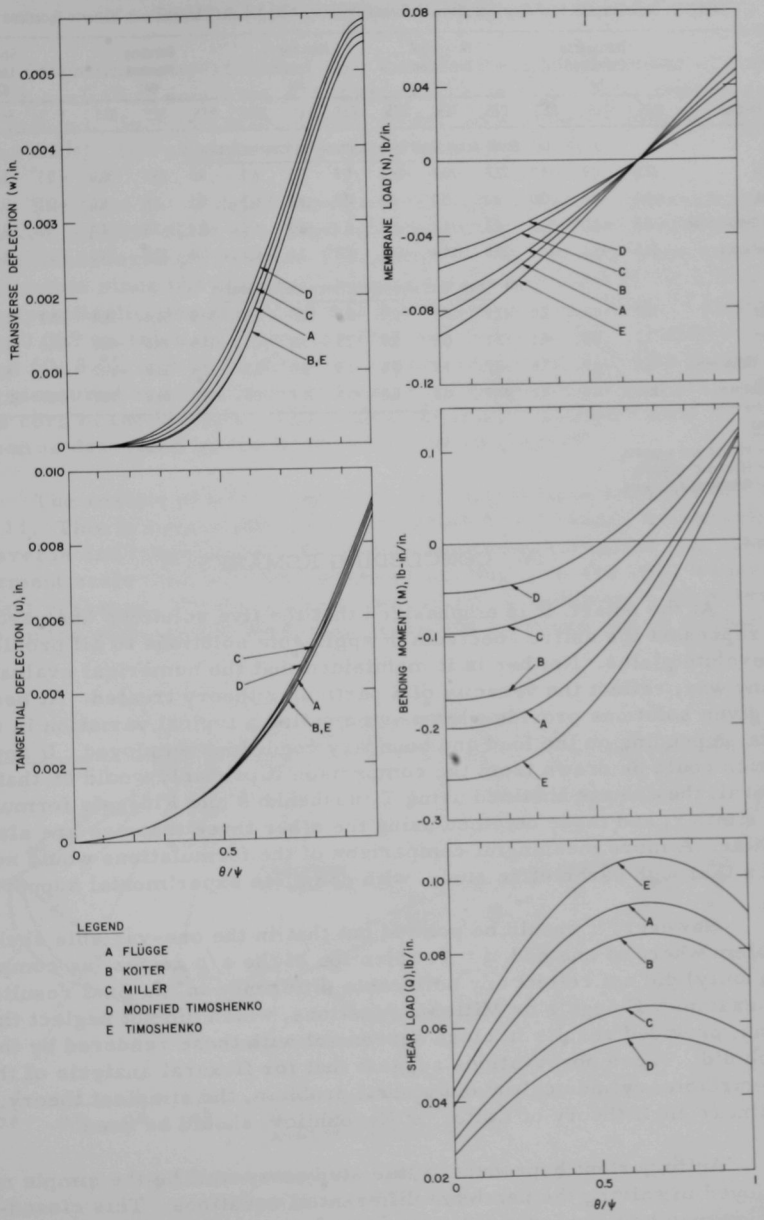

Fig. 10. Variation in Displacement and Internal Load of Involute Shell Which Has Rotated End Supports and Is Subjected to Isothermal Expansion

TABLE 3. Deviations (in %) of Four Solutions of Sample Problems from Results Obtained with Koiter's Equations

Method	Transverse Deflection (w)			Tangential Deflection (u)			Membrane Load (N)			Bending Moment (M)			Shear Load (Q)		
	PES	FES	RES	PES	FES	RES	PES	FES	RES	PES	FES	RES	PES	FES	RES
(A) Shell Acted Upon by a Uniform Transverse Pressure															
Flügge	12.0	- 8.9	-14.2	22.8	-20.7	-28.1	-0.3	2.3	6.3	- 0.9	25.1	30.0	- 0.3	5.4	- 6.5
Miller	- 0.1	0.2	0.0	0.0	0.0	0.0	0.0	0.0	0.1	0.1	0.0	0.0	- 0.1	-0.1	0.0
Mod. Timoshenko	- 3.3	- 1.0	- 2.5	-4.2	- 1.3	- 2.7	0.0	-0.3	-5.7	- 0.4	-1.9	- 4.0	- 0.2	-0.4	0.1
Timoshenko	11.5	-13.1	-13.1	23.9	-14.8	-13.1	-0.3	2.6	6.3	- 0.8	27.5	30.0	- 0.3	6.7	- 6.5
(B) Shell Restrained from Isothermal Expansion															
Flügge	-17.7	0.2	2.0	47.7	- 0.6	2.0	-5.0	22.0	1.0	-50.0	56.4	18.4	-50.1	24.7	10.1
Miller	- 1.2	0.6	4.1	2.1	- 0.8	3.8	-1.5	3.8	-2.3	-14.9	10.5	-42.9	-15.2	4.2	-23.5
Mod. Timoshenko	- 1.4	0.9	5.6	-0.7	- 1.7	5.4	-1.3	8.0	-3.3	-12.8	13.8	-69.0	-12.8	8.5	-33.1
Timoshenko	-16.6	0.0	0.2	43.9	- 0.3	0.0	-3.5	19.7	2.5	-34.8	49.0	50.7	-34.9	22.3	24.6

Legend

PES - Pinned end supports.
FES - Fixed end supports.
RES - Rotated end supports.

IV. CONCLUDING REMARKS

At the outset, it is emphasized that the five solutions analyzed do not represent the entire spectrum of applicable solutions to all problems of involute plates. Neither is it maintained that the numerical evaluations, in any way, reflect the veracity of a particular theory treated. At best, the given solutions provide what may be called a typical variation in results, depending on the load and boundary conditions employed. If any conclusion could be drawn from the comparison it probably would be that, in general, the results obtained using Timoshenko's and Flügge's formulations are similar, and those obtained using the other three theories are also similar. A more meaningful comparison of the formulations would necessitate a thorough parametric study, with complete experimental support.

However, it should be pointed out that in the one-variable shell problem where at one end $\rho = 0$, retention of the z/ρ terms (as compared with unity) did not reflect any noticeable difference in the final results. For example, Flügge's or Miller's equations, which did not neglect the z/ρ terms, provided results in close agreement with those rendered by theories which did. These observations suggest that for flexural analysis of the two-variable, cylindrical involute shell problem, the simplest theory, say the linear shell theory of Koiter or Novozhilov, should be used.

An important byproduct of this study may well be the simple method employed in solving the pertinent differential equations. This closed-form solution may be used for quantitative comparisons, since the one-dimensional model still retains many of the relevant characteristics of interest.

V. COMPARISON WITH EXPERIMENTAL DATA

Oftentimes experimental data are available for purposes of comparison with analytical solutions, but may not always completely represent the study at hand. Such is the case with the two sets of data furnished by the staff at ORNL, and allowances must be made accordingly.

The first set of data* consisted of displacement measurements on a simulated involute plate specimen, with pinned (or grooved) ends, subjected to uniform transverse pressures. (The shape of the test specimen was not a true involute since the ends had straight extensions, each about 1/8 in. long.) More specifically, the specimen was fabricated of Type 6061-T6 aluminum sheet, 0.039 in. thick, the cord of which was 3.372 in. long. Pressures of 3.63, 5.60, 8.54, and 10.51 psi were applied, and corresponding displacements were measured at seven stations by dial indicators positioned perpendicular to the cord of the involute. The equivalent analytical shape used for comparison is described by the input conditions on page 25.

The results of this comparison are summarized and replotted in Fig. 11. This is essentially a two-dimensional plot, where the experimental transverse and tangential displacements have been accounted for. The displacement scale also was normalized by plotting w/p and u/p, where p is the test pressure. This normalization permitted inclusion of all pressure results on the same graph. Since the analytical solutions can be divided into

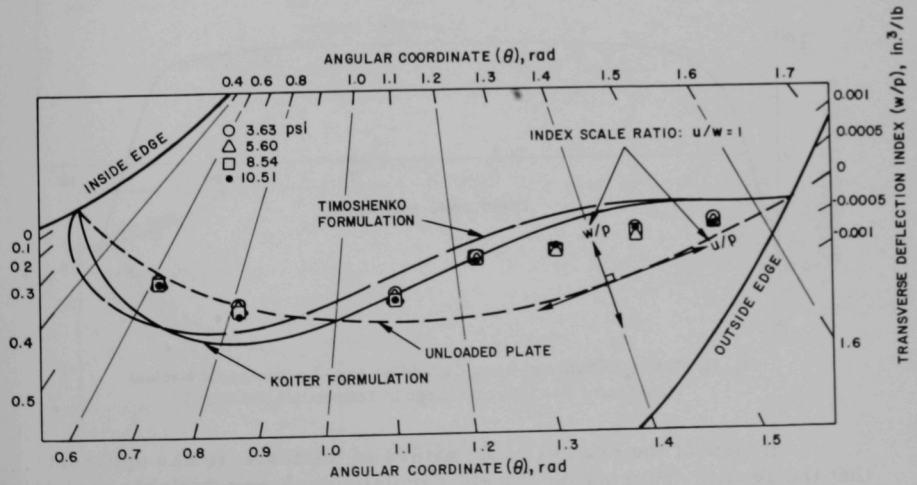

Fig. 11. Comparison of Experimental Data with Analytical Results for Shell with Pinned Edges and Subjected to Uniform Pressure

*Personal communication from T. G. Chapman, ORNL.

two groups insofar as agreement between them is concerned, Koiter's and Timoshenko's solutions have been plotted for comparison. Their disagreement with the experimental results is quite apparent; however, of the two solutions, that rendered by Koiter's formulation is in somewhat closer agrement with experiment.

The second set of data was derived by Cheverton and Kelley,[3] who conducted a series of experiments on plates of the HFIR outer fuel element. Structurally, each test specimen was a cylindrical, aluminum involute plate, 0.050 in. thick, with a generating circle of 5.873 in., a true active width (arc length) of 2.944 in., and an axial length of 24 in.

Numerous variables, such as types of material, restraints of the side supports, and type of load, were considered in these tests. One of the test objectives was to reproduce, as closely as possible, the true structural loads and restraints on the plates. For example, the higher temperature environment of the plate, as compared to its restraining boundaries, was simulated by effectively imparting an axial shear load on the sides of the plate. Figure 12 shows the maximum transverse deflection incurred along the cylinder axis under these conditions. In tests where pressure was to be applied to the plate surface, the entire perimeter of the plate was sealed. The mode of sealing prevented the ends of the plates from deforming under load, as they would under actual operating conditions.

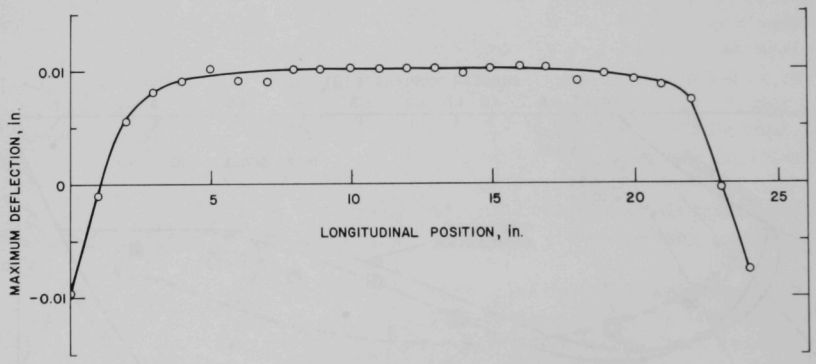

Fig. 12. Typical Deformation along Cylindrical Axis of a Free-ended Involute Plate Caused by a Uniform Change in Temperature (80-400°F)

In view of the multivariable nature of the tests, it was apparent that the results could not be closely simulated by a one-variable analytical model. However, it was believed that a reasonable comparison could be made with displacements measured along the involute and at the midlength of the plates (see Fig. 12). Accordingly, data derived from conditions of

fixed edges of the plate were selected. In these tests, the plate temperature was increased from 80 to 400°F, with no pressure differential; at 400°F, pressure was applied to the plate surface.

The results of the comparisons are plotted in Figs. 13 to 15. Here again, the analytical results were derived using the Timoshenko and Koiter formulations, and the physical properties of aluminum at elevated temperatures as published in Sect. III of the ASME Boiler and Pressure Vessel Code. Figure 13 shows the plate deformation caused by the isothermal temperature change from 80 to 400°F. The configuration of deformation is similar to that determined analytically, but the quantitative values do not

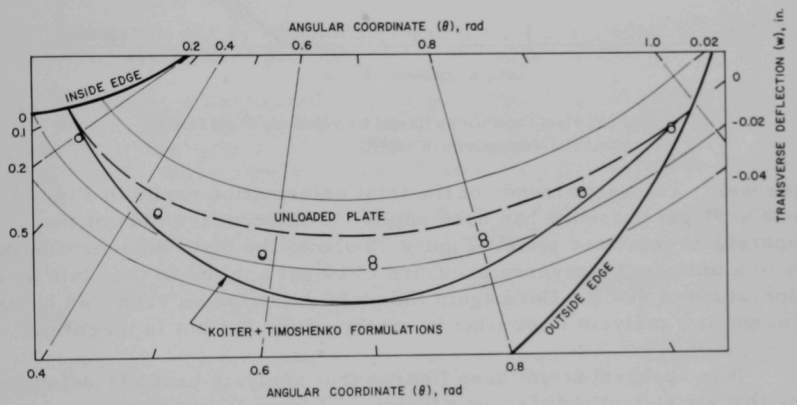

Fig. 13. Deformation of Involute Plate Caused by an Isothermal Temperature Change (80-400°F)

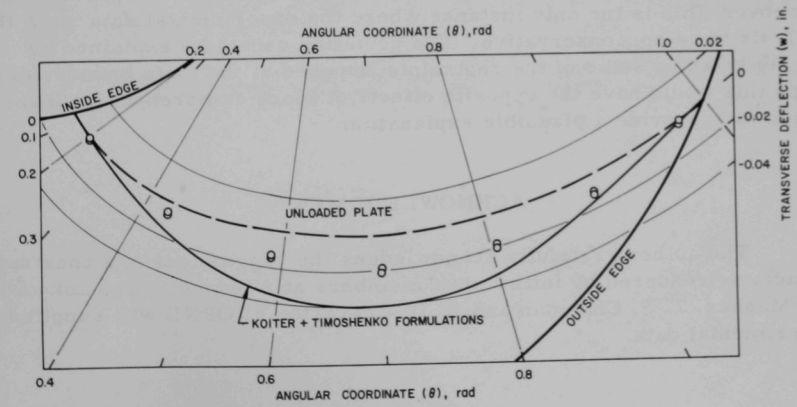

Fig. 14. Plate Deformation Caused by an Isothermal Temperature Change (80-400°F) and a Uniform Pressure of 30 psi

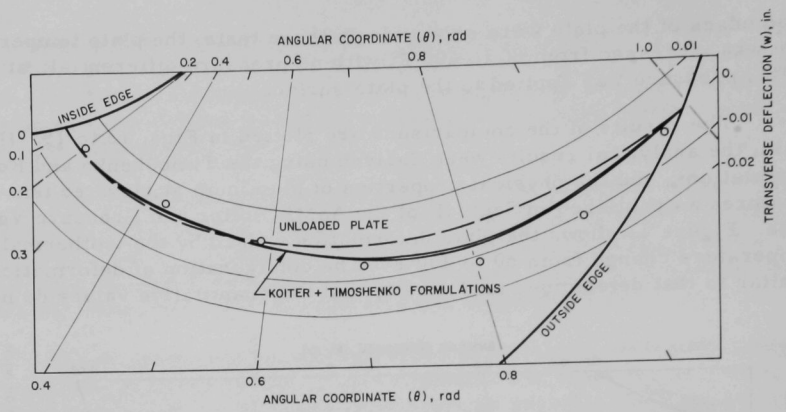

Fig. 15. Plate Deformation Caused by a Uniform 60 psi Pressure at a Temperature of 400°F

agree well. The same trends of the total deformation occur in Fig. 14, where a 30-psi pressure has been applied to the concave side of the temperature-deformed plate. Figure 15 shows the plate deformation due only to a uniform transverse pressure of 60 psi applied to the plate at a temperature of 400°F. Here again the plate deformation rendered by experiment and analysis is similar in configuration but not in magnitude.

It is apparent from these figures that analysis predicts deformations that consistently differ by a factor of 2 from those determined experimentally. Of particular importance is the fact that the analytically derived deformations due to transverse pressure (see Fig. 15) are nonconservative: predicted plate deflections are lower than those measured experimentally. Moreover, this is the only instance where the experimental data show the analysis to be nonconservative. The deviation cannot be explained by simply relaxing some of the restraints imposed at the plate boundaries, since this would have the opposite effect. A more comprehensive investigation may provide a plausible explanation.

ACKNOWLEDGMENT

The author gratefully acknowledges the suggestions and constructive criticisms rendered by fellow staff members at Argonne. Also acknowledged are Messrs. T. S. Chapman and R. D. Cheverton of ORNL who supplied the experimental data.

REFERENCES

1. L. W. Fromm *et al.*, *Preliminary Safety Analysis Report on the Argonne Advanced Research Reactor*, ANL-7448 (June 1968).

2. J. R. McWherter and T. G. Chapman, *Mechanical and Hydraulic Design of the HFIR*, Research Reactor Fuel Element Conference, Gatlinburg, Tenn., September 17-19, 1962, TID-7642, Bk. 1, p. 99.

3. R. D. Cheverton and W. H. Kelley, *Experimental Investigation of HFIR Fuel Plate Deflections Induced by Temperature and Pressure Differentials*, ORNL-TM-2325 (Aug. 16, 1968).

4. S. Timoshenko and S. Woinowsky-Krieger, *Theory of Plates and Shells*, 2nd ed., McGraw-Hill Book Co., Inc., New York (1959).

5. W. T. Koiter, *A Consistent First Approximation in the General Theory of Thin Elastic Shells*, Proc., Symposium on the Theory of Thin Elastic Shells, Technological Univ. of Delft, The Netherlands, 1959, (ed.) W. T. Koiter, North-Holland Publishing Co., Amsterdam (1960).

6. A. E. H. Love, *A Treatise on the Mathematical Theory of Elasticity*, 4th ed., Dover Publications, New York (1944).

7. V. V. Novozhilov, *The Theory of Thin Shells*, P. Noordhoff, N. V., Groningen, The Netherlands (1959).

8. E. Reissner, *A New Derivation of the Equations for the Deformation of Elastic Skells*, Amer. J. Math., *53*, 177-184 (1941).

9. W. Flügge, *Stresses in Shells*, Springer-Verlag, Inc., New York (1966).

10. R. E. Miller, *Theory of Nonhomogeneous Anisotropic Elastic Shells Subjected to Arbitrary Temperature Distribution*, Univ. of Ill. Engrg. Expt. Station Bulletin No. 458 (1960).

11. J. L. Sanders, Jr., *An Improved First Approximation Theory for Thin Shells*, NASA Technical Report R-24 (1959).

ARGONNE NATIONAL LAB WEST
3 4444 00011538 6